Int. J. Electrochem. Sci., 14 **(2019)** 9520 – 9526, doi: 10.20964/2019.10.17

International Journal of
ELECTROCHEMICAL
SCIENCE
www.electrochemsci.org

Short Communication

S@NiS Hollow Spheres as Cathode Materials for Lithium-Sulfur Batteries

Bing Che[*], *Dong Wang*[*], *Xiaochun Xu*

State Grid Huaian Power Supply Company, Huaian 223002, Jiangsu, China, P.R.
[*]E-mail: che3510@sina.com, 15061217411@163.com

Received: 1 June 2019 / *Accepted:* 11 July 2019 / *Published:* 30 August 2019

Severe capacity fading substantially hinders the employment of lithium-sulfur batteries in the electric vehicles. This is primarily due to the shuttle effect of the polysulfide in the electrolyte. Therefore, the most efficient method to improve the cycle stability of the lithium-sulfur batteries is inhibiting the shuttle effect of the polysulfide in the electrolyte. To deal with this problem, S@NiS hollow sphere composites are synthesized and employed as cathode materials in lithium-sulfur batteries. This unique hollow structure could serve as a storage device for the soluble polysulfides. As a result, the electrochemical performance of the lithium-sulfur battery is greatly enhanced by using S@NiS hollow spheres composites.

Keywords: S@NiS, hollow spheres, composites, Li-S battery

1. INTRODUCTION

Lithium-sulfur batteries are one of the most promising candidates for the next generation energy storage systems for the electric vehicles worldwide, because of their high specific capacity (1675 mAh g^{-1}) and energy density (2600 Wh Kg^{-1}) of the lithium-sulfur batteries [1, 2, 3]. It is three times higher than the traditional lithium-ion batteries [4, 5]. Therefore, lithium-sulfur batteries have been receiving much attention from the researchers in recent decades.

The works involving lithium-sulfur batteries mainly includes the following: a) developing cathode host materials for the sulfur particles, b) coating the PP separator with various functional materials, c) protecting the lithium anode by using lithium alloy. All of above works are reported to improve the cycle stability and capacity value of the lithium-sulfur batteries [6, 7, 8]. Lithium-sulfur batteries suffer from severe capacity fading during the electrochemical process, which is mainly caused by the migration of the soluble polysulfide between the cathode and anode side [9, 10]. Consequently, the migration of the polysulfide must be inhibited during the discharging and charging process [11,

12].

In this paper, hollow S@NiS sphere composites are developed and designed as cathode materials for the lithium-sulfur batteries. This unique hollow sphere structure could provide a place for the storage of the soluble polysulfide. Therefore, the shuttle effect of the polysulfide in the lithium-sulfur battery could be effectively inhibited during the discharging and charging process. As a result, the hollow S@NiS composites show excellent cycle stability and high specific capacity. In all, this work may provide a promising method for synthesizing the cathode materials for the lithium-sulfur batteries.

2. EXPERIEMENTAL

2.1. Preparation of the hollow S@NiS composites

Typically, 2.6 g $Na_2S_2O_3$ $5H_2O$ was added into the 10 ml HCl solution under stirring. The solution was named solution A. At the same time, 0.5 g $NiSO_4$ $6H_2O$ and 0.3 g Na_2S $9H_2O$ were added into polyethylene glycol solution, separately. The obtained solutions were named solution B and C, respectively. After that, the solution A and B were mixed together. Then, the solution C was added into the above mixed solution drop and drop under magnetic stirring for 30 min. Finally, the solid substrate was washed and collected. The obtained sample is the hollow S@NiS sphere composites.

2.2. Materials Characterization

The morphologies of the samples were observed by using scanning electron microscopy (SEM, SIGMA 500) and transmission electron microscopy (TEM, JEM-F200). The sulfur content in the composites was tested by using TG analysis (TG, DZ3339).

2.3. Electrochemical Performance

The electrochemical performance of the samples was tested by assembling coin 2016 half batteries. The electrode slurry was firstly prepared by mixing S@NiS composites, carbon black and PVDF with a ratio of 8:1:1. The as-prepared S@NiS electrodes were used as cathode and counter electrode. The lithium was used as anode. The model of the separator is Celgard 2300. The electrolyte consists of 1M LiTFSI with DOL:DME=1:1. Discharge/charge profiles were tested on the battery tester (LAND CT2001A) between 1.5 V and 3.0 V.

3. RESULTS AND DISCUSSION

Figure 1a shows the morphology of the hollow NiS spheres. It can be clearly seen that the NiS materials had a hollow sphere structure with a dimeter of 100-120 nm. Furthermore, the morphology of S@NiS composites was observed with scanning electron microscope [13, 14]. As shown in Figure 1b,

the S@NiS composites had a similar morphology with the pure NiS spheres. This demonstrates that the sulfur particles are fully immersed into the hollow structure of the NiS hollow spheres. To further confirm the successful preparation of the S@NiS composites, EDS was conducted for the S@NiS composites. As shown in Figure 1c-e, it can be observed that the elements Ni and S are uniformly dispersed in the whole S@NiS composites [15]. The uniform distribution in the whole composites is beneficial for the release of the capacity during the discharging and charging processes.

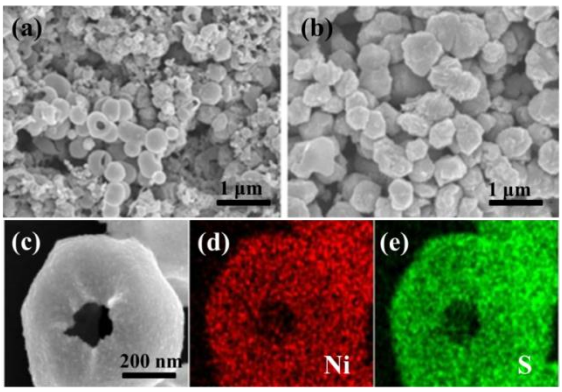

Figure 1. (a) SEM image of NiS hollow spheres, (b) and (c) SEM image of S@NiS hollow spheres composites.(d) and (e) Corresponding elemental mapping of Ni and S for the S@NiS hollow spheres composites.

The TEM images of the NiS hollow spheres and S@NiS composites are shown in Figure 2. As shown in Figure 2a and b, the NiS spheres had a hollow structure with sufficient internal space [16]. This hollow space could act as a storage device for the sulfur particle and polysulfide. As a result, the hollow structure could inhibit the shuttle effect of the polysulfide during the electrochemical process. Figure 2c and d are the TEM images of the S@NiS spheres composites. From the figure, it can be seen that the internal space in the NiS hollow spheres is occupied with the sulfur particles [17]. This clearly indicates that the S@NiS hollow spheres are successfully prepared.

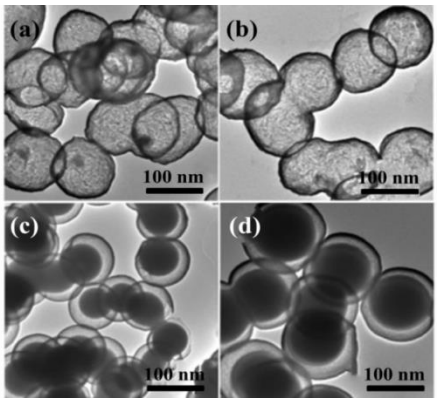

Figure 2. TEM images of (a) and (b) NiS hollow spheres, (c) and (d) S@NiS hollow spheres composites.

Figure 3a shows the XRD pattern of the S@NiS-HS composites. As shown in Figure 3a, the as-

prepared S@NiS-HS composites exhibit typical diffraction peaks of the sublimed sulfur. The main sulfur diffraction peaks in the S@NiS-HS composite indicate that the strong sulfur peaks cover the peaks of the NiS. Therefore, the peaks of the NiS are nearly invisible. Overall, the XRD pattern of the S@NiS-HS composites confirms the successful preparation of the S@NiS-HS. This result is consistent with the previous TEM result [18, 19]. To obtain the sulfur content in the S@NiS-HS composites, TG analysis was conducted for the S@NiS-HS composites. As shown in Figure 3b, the weight loss occurs at the 310ºC, which means the sublimation of the element sulfur in the S@NiS-HS composites. It can be clearly seen that the sulfur content is approximately 68% in the S@NiS-HS composites. This sulfur content is used for calculating the specific capacity of the as-prepared S@NiS cathode materials [20].

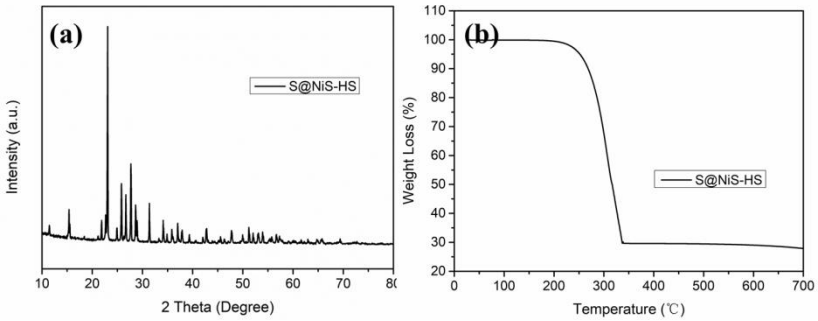

Figure 3. (a) The XRD pattern of the S@NiS-HS composites. (b) TG curves of the S@NiS-HS composites.

To study the chemical components and bonding in the S@NiS-HS composites, XPS was conducted for the S@NiS-HS composites, as shown in Figure 4. Figure 4a shows the S 2p for the S@NiS-HS composites. Two peaks at 164.3 eV and 169.1 eV, respectively. These two peaks are corresponding to the S $2p_{3/2}$ and S $2p_{1/2}$, respectively. The XPS of the Ni 2p is shown in Figure 4b. The peaks at 852.5 eV and 867.3 eV are related to the Ni^0 $2p_{3/2}$ and Ni ^{0} $2p_{1/2}$. Furthermore, the peak at 857.3 eV corresponds to the Ni^{2+} $2p_{3/2}$, which confirms the presence of the Ni^{2+}. Moreover, the peak at 877.1 eV is corresponding to the Ni-S bond between the NiS and element sulfur in the S@NiS-HS composites.

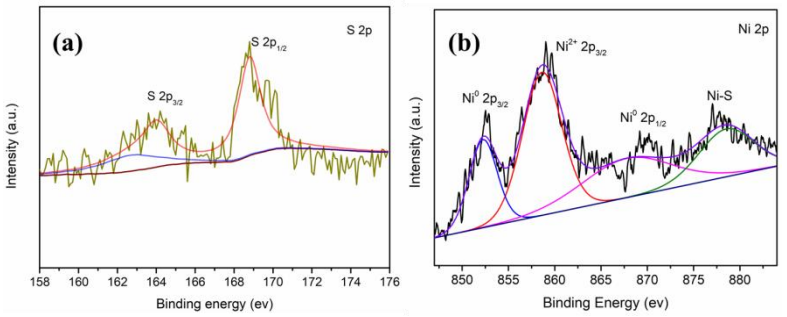

Figure 4. The XPS of the S@Ni-S-HS composites for the (a) S 2p and (b) Ni 2p.

Figure 5 shows the DC curves of the S@NiS-HS composite electrode and sulfur electrode at the current density of 0.1 C. It can be obtained following information: a) the capacity value for the

S@NiS-HS composite electrode is much higher than the sulfur electrode. The initial specific capacity of the S@NiS-HS composite electrode is as high as 1506 mAh g^{-1} at the current density of 0.1 C. However, the first specific capacity is only 1100 mAh g^{-1} for the sulfur electrode. b) Two voltage platforms can be observed at 2.3 V and 2.1 V, respectively. Especially, the plateau at 2.1 V provides main capacity contribution, which is related to the change from the soluble polysulfide to the Li_2S. Therefore, the specific capacity of the lithium-sulfur battery could be enhanced by using hollow NiS spheres as host materials for the element sulfur [21, 22].

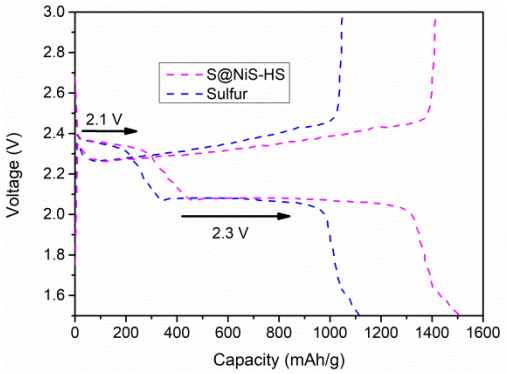

Figure 5. The constant discharging and charging profiles of the S@NiS-HS composite electrode and sulfur electrode at the current density of 0.1 C.

Figure 6 shows the rate performance of the S@NiS-HS composite electrode and sulfur electrode at various current densities from 0.1 C to 2 C. It can be seen that the S@NiS-HS electrode shows superior rate performance during the increase of the current densities. Even at the high current density of 2 C, the specific capacity of the S@NiS-HS electrode is as high as 986 mAh g^{-1}, which is much higher than that of the pure sulfur electrode. Therefore, the as-prepared S@NiS-HS electrode could withstand a change in the current densities. However, for the pure sulfur electrode, the specific capacity fades rapidly with the increase of the current densities, demonstrating a poor rate capability.

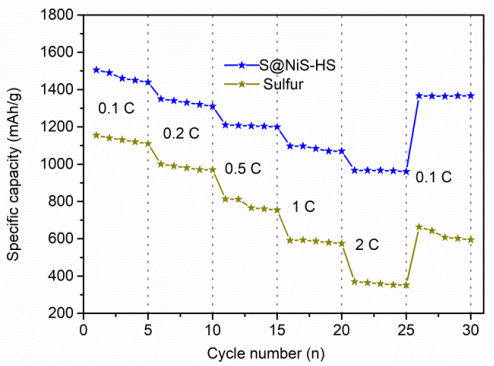

Figure 6. The rate capability of the S@NiS-HS composite electrode and sulfur electrode.

To further investigate the electrochemical performance of the S@NiS-HS electrodes, long cycle performance was tested at a current density of 0.5 C for 100 cycles. As shown in Figure 7, the S@NiS-HS electrode shows an initial specific capacity of 1106 mAh g^{-1} at a current density of 0.5 C. The specific capacity of the S@NiS-HS electrode still remains at 908 mAh g^{-1} after 100 cycles. The capacity retention of the S@NiS-HS electrode is as high as 82%, which is much higher than that of the other similar cathode materials. For the pure sulfur electrode, the capacity value is much smaller than the S@NiS-HS electrode. Moreover, the capacity of the pure sulfur electrode decreases rapidly with the increasing cycle numbers.

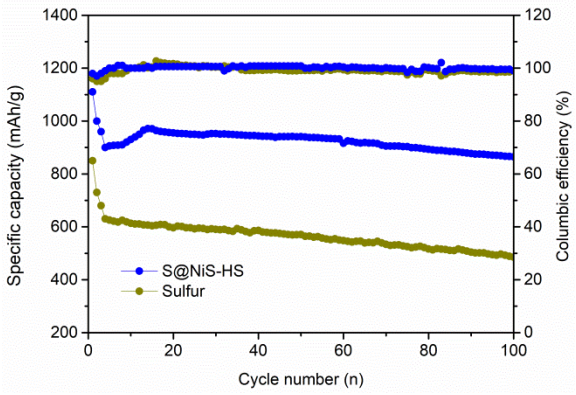

Figure 7. The cycle performance of the S@NiS-HS composite electrode and sulfur electrode at the current density of 0.5 C.

Table 1. The electrochemical performance of the S@NiS hollow spheres compared with other reported similar cathode materials for the lithium-sulfur batteries.

Electrodes	Current Density	Capacity	References
SnO_2/C-S	0.1 C	785 (80 cycles)	24
S-V_2O_3	0.2 C	568 (100 cycles)	25
ZIF@S@MnO_2	0.5 C	895 (100 cycles)	26
S@NiS	0.5 C	908 (100 cycles)	This Work

4. CONCLUSIONS

In summary, hollow S@NiS sphere composites were synthesized and used as cathode materials for the lithium-sulfur batteries. The S@NiS composites show high specific capacity and superior cycle stability during the discharging and charging process. This is ascribed to the unique hollow spheres structure, which could act as a capsule for the storage of the soluble polysulfide. The initial specific capacity of the S@NiS-HS composite electrode is as high as 1506 mAh g^{-1} at a current density of 0.1 C.

ACKNOWLEDGEMENT
We thank the financial support from the State Grid Huaian Power Supply Company.

References

1. Y. Li, J. Chen, Y. F. Zhang, Z. Y. Yu, T. Z. Zhang, W. Q. Ge and L. P. Zhang, *J. Alloy Compd*., 766 (2018) 804.
2. M. D. Walle, K. Zeng, M. Y. Zhang, Y. J. Li and Y. N. Liu,, *Appl. Surf. Sci*., 473 (2019) 540.
3. H. J. Zhao, N. P. Deng, J. Yan, W. M. Kang, J. G. Ju, Y. L. Ruan, X. Q. Wang, X. P. Zhuang, Q. X. Li and B. W. Cheng, *Chem. Eng. J*., 347 (2018) 343.
4. X. Dong, Z. P. Deng, L. H. Huo, X. F. Zhang and S. Gao, *J. Alloy Compd*., 788 (2019) 984.
5. Z. J. Liu, B. L. Liu, P. Q. Guo, X. N. Shang, M. Z. Lv, D. Q. Liu and D. Y. He, *Electrochim. Acta*, 269 (2018) 180.
6. S. P. Wu, R. Y. Ge, M. J. Lu, R. Xu and Z. Zhang, *Nano Energ*., 15 (2015) 379.
7. C. Y. Jin, L. P. Zhou, L. C. Fu, J. J. Zhu, D. Y. Li and W. L. Yang, *J. Power Sources*, 352 (2017) 83.
8. H. W. Tang, C. X. Zhang, K. Chang, S. G. Enbao, B. Li, Z. R. Chang, *Int. J. Hydorgen Energ*y, 42 (2017) 24939.
9. Q. C. Chen, S. B. Ni, J. Tang, T. Li, T. Kang and X. L. Yang, *Mater. Lett*., 213 (2018) 193.
10. X. Y. Li, Y. M. Chen, J. Z. Zou, X. R. Zeng, L. M. Zhou and H. T. Huang, *J. Power Sources*, 331 (2016) 360.
11. M. Li, J. B. Zhou, J. Zhou, C. Guo, Y. Han, Y. C. Zhu, G. M. Wang and Y. T. Qian, *Mater. Res. Bull*., 96 (2017) 509.
12. X. Y. Wu, S. M. Li, Y. Y. Xu, B. Wang, J. H. Liu and M. Yu, *Chem. Eng. J*., 356 (2019) 245.
13. H. C. Ruan, Y. F. Li, H. Y. Qiu and M. D. Wei, *J. Alloy Compd*., 588 (2014) 357.
14. L. J. Liu, Y. Chen, Z. F. Zhang, X. L. You, M. D. Walle, Y. J. Li and Y. N. Liu, *J. Power Sources*, 325 (2016) 301.
15. K. Aso, A. Hayashi and M. Tatsumisago, *Electrochim. Acta*, 83 (2012) 448.
16. X. L. Li, K. Zhao, L. Y. Zhang, Z. Q. Ding and K. Hu, *J. Alloy Compd*., 692 (2017) 40.
17. J. Balach, T. Jaumann and L. Giebeler, *Energ. Storage Mater*., 8 (2017) 209.
18. Q. Zhang, S. Bolisetty, Y. Cao, S. Handschin, J. Adamcik, Q. Pengand R. Mezzenga, Angew. Chem. Int. Edit., 58 (2019), 6012.
19. N. Li, S. F. Tang, Y. D. Rao, J. B. Qi, Q. R. Zhang, D. L. Yuan, *Electrochim. Acta* 298 (2019) 59.
20. L. L. Fan, N. P. Deng, J. Yan, Z. H. Li, W. M. Kang and B. W. Cheng, *Chem. Eng. J*., 369 (2019) 874.
21. J. Pu, Z. H. Shen, J. X. Zheng, W. L. Wu, C. Zhu, Q. W. Zhou, H. G. Zhang and F. Pan, *Nano Energ*., 37 (2017) 7.
22. Z. Li, S. F. Deng, H. J. Li, H. Z. Ke, D. L. Zeng, Y. F. Zhang, Y. B. Sun H. S. Cheng, 347 (2017) 238.
23. S. Z. Zeng, Y. C. Yao, X. R. Zeng, Q. J. He, X. F. Zheng, S. S. Chen, W. X. Tu and J. Z. Zou, *J. Power Sources*, 357 (2017) 11.
24. M. L. Qi, X. Q. Liang, F. Wang, M. S. Han, J. H. Yin, M. H. Chen, *J. Alloy Compd*., 799 (2019) 345.
25. M. Q. Zhu, S. M. Li, J. H. Liu and B. Li, *Appl. Surf. Sci.*, 473 (2019) 1002.
26. K. Wang, W. Y. Li, W. K. Ye, W. H. Yin, W. W. Chai, Y. Qu and Y. C. Rui, *J. Alloy Compd*., 793 (2019) 16.